Florian Straube, Frank Schultz, David Albanés Bonillo, Stefan Weinzierl

An Analytical Approach for Optimizing the Curving of Line Source Arrays

Citation details
Straube, Florian; Schultz, Frank; Bonillo, David Albanés; Weinzierl, Stefan (2018). An Analytical Approach for Optimizing the Curving of Line Source Arrays. J. Audio Eng. Soc., vol. 66, no. 1/2, pp. 4–20. https://doi.org/10.17743/jaes.2017.0043.

An Analytical Approach for Optimizing the Curving of Line Source Arrays

FLORIAN STRAUBE, *AES Associate Member*, **FRANK SCHULTZ,** *AES Associate Member*,
(florian.straube@tu-berlin.de) (frank.schultz@tu-berlin.de)

DAVID ALBANÉS BONILLO, AND STEFAN WEINZIERL
(davidalbanes@gmail.com) (stefan.weinzierl@tu-berlin.de)

Audio Communication Group, TU Berlin, DE-10587 Berlin, Germany

Line source arrays (LSAs) are used for large-scale sound reinforcement aiming at the synthesis of homogeneous sound fields for the whole audio bandwidth. The deployed loudspeaker cabinets are rigged with different tilt angles and/or are electronically controlled in order to provide the intended coverage of the audience zones and to avoid radiation towards the ceiling, reflective walls or residential areas. This contribution introduces the analytical polygonal audience line curving (PALC) approach for finding appropriate LSA cabinet tilt angles with respect to the geometry of the receiver area and the intended coverage. PALC can be applied in advance of a numerical optimization of the loudspeakers' driving functions. The method can be used with different objectives, such as a constant interaction between adjacent cabinets with respect to the receiver geometry or by additionally considering amplitude attenuation over distance. PALC is compared with typical standard LSA curving schemes. The advantages of the presented approach regarding sound field homogeneity and target-oriented radiation are evaluated based on technical quality measures.

0 INTRODUCTION

For the optimization of the curving and the electronic control of line source arrays (LSAs) for advanced sound reinforcement there is no standard procedure. In practice, both a pure geometric and a pure electronic wavefront shaping as well as combinations thereof are realized. Even state-of-the-art line array systems with extensive beam steering capabilities differ significantly [1]. Since they comprise several individually controllable, small drivers, beam steering is feasible up to high audio frequencies. While the cabinets of some array systems are curved in addition to the beam steering, the cabinets of other systems are rigged as a straight line.

Recent, mostly proprietary software such as Martin Audio Display [2], EAW Resolution 2 [3], d&b ArrayCalc [4], and AFMG FIRmaker [5] offer (numerical) optimization schemes but the algorithms and the parametrization are rarely publicly documented. In the literature the calculation of appropriate driving signals, i.e., finite impulse response (FIR) filters for the individual LSA loudspeakers in order to generate a desired sound field by numerical optimization techniques, was discussed in [6–12]. These approaches yield considerable improvements with respect to homogeneous audience coverage and/or avoidance of high side lobe energy compared to manually adjusted setups. In [8, 10, 13] also the LSA cabinet tilt angles are determined by numerical optimization methods. The established Wavefront Sculpture Technology (WST) criteria for LSAs [14, p. 929] also comprise a geometrical criterion for audience coverage considering the splay angles between LSA cabinets and the source-to-receiver distances.

As the process for combined geometric-electronic optimization typically starts with the curving, this article is only focused on finding optimal tilt angles. These could be taken as a pre-processing stage for the optimization of the loudspeakers' driving functions, i.e., for the calculation of the FIR filter coefficients, or could also be applied for uniformly driven line arrays without further computation.

In this article we aim at introducing the analytical polygonal audience line curving (PALC) approach for finding appropriate LSA cabinet tilt angles with respect to the geometry of the receiver area and the intended coverage. The method can be used with different objectives, such as a constant interaction between adjacent cabinets with respect to the receiver geometry or by additionally considering amplitude attenuation over distance, i.e., sound pressure level (SPL) loss over distance. PALC is evaluated in comparison with typical standard LSA curving schemes (straight, arc, J, progressive, numerically optimized). Acoustic simulations based on the complex-directivity point source (CDPS) model [6, 15–17] including far-field radiation patterns

Table 1. List of abbreviations.

ARF	active radiating factor
ATF	acoustic transfer function
BEM	boundary element method
CDPS	complex-directivity point source
FIR	finite impulse response
HF	high frequency
LF	low frequency
LSA	line source array
MA	Martin Audio
MF	mid frequency
MZSFS	multi-zone sound field synthesis
PAL	polygonal audience line
PALC	polygonal audience line curving
PIP	position index plot
prog	progressive array
SPL	sound pressure level
str	straight array
WST	Wavefront Sculpture Technology

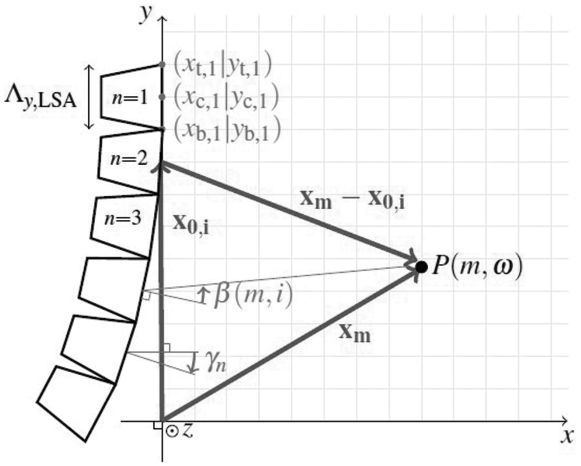

Fig. 1. Sketch of the LSA setup under discussion. A total of $N = 16$ LSA cabinets of the height $\Lambda_{y,\mathrm{LSA}} = 0.372$ m is used. See Table 11 and Table 12 for the deployed tilt angles γ_n.

of baffled line and circular pistons provide the basis for an evaluation of the introduced approach. One uniformly driven LSA model is analyzed for two concert venues.

The article is organized as follows. In Sec. 1 the chosen LSA model and the selected concert venues are presented. Mathematical fundamentals—among them especially the adjusted CDPS model—are shortly revisited in Sec. 2. In Sec. 3 the established WST approach is considered and the PALC algorithm is described. The evaluation criteria and the results for the different LSA curving schemes are shown in Sec. 4 and are discussed in Sec. 5. In Table 1 frequently used abbreviations of this article and in the Appendix in Table 2, Table 3, Table 4, Table 5 as well as in Table 6 frequently used mathematical variables of this article are arranged with regard to their application and formalism.

1 SIMULATION SETUP

An LSA setup is examined for two concert venues following practical examples presented in [10, Sec. 6.1] and in [18, Sec. 4.2.2] with audience and non-audience sections given within the vertical LSA radiation plane, i.e., the *xy*-plane in this case. While the first location is a typical multi-stand arena, the second one resembles a common open-air amphitheater geometry.

1.1 Line Source Array Setup

The LSA setup and the geometry under discussion are schematically depicted in Fig. 1 for calculating the sound pressure $P(m, \omega)$ at the m-th receiver position characterized by the vector $\mathbf{x_m}$ at the angular frequency ω. A total of $N = 16$ LSA cabinets with $n = 1, 2, ..., N$ is deployed. The front grille's height $\Lambda_{y,\mathrm{LSA}}$ of a single LSA cabinet is set to 0.372 m resulting in an overall LSA length of ca. 5.96 m. γ_n denotes the individual tilt angle of the n-th LSA cabinet and $\mathbf{x_{0,i}}$ denotes the vector of the front grille center position of the i-th LSA driver. The vectors $\mathbf{x_{t,n}}$, $\mathbf{x_{c,n}}$ and $\mathbf{x_{b,n}}$ define the top, center, and bottom position of the n-th LSA cabinet, respectively. With the radiation angle $\beta(m, i)$, the source-receiver configuration is specified for the i-th source and the m-th receiver position. Detailed information on the geometric setup can be found in [19, 20].

Built from three-way cabinets in this article, the exemplarily chosen LSA consists of $V_{\mathrm{LF}} = 1$, $V_{\mathrm{MF}} = 4$ and $V_{\mathrm{HF}} = 10$ vertically stacked, individually controlled drivers per cabinet for the low, the mid, and the high frequency band (LF, MF, HF). 12-inch, 3-inch, and 1.2-inch speakers are used for LF, MF, and HF, respectively. Thus, the LSA consists of a total of VN sources with $i = 1, 2, ..., VN$ for each frequency band.

Different frequency independent loudspeaker sensitivities are assumed in order to obtain realistic sound pressure values, $S_{\mathrm{LF}} = 96$ dB, $S_{\mathrm{MF}} = 88$ dB and $S_{\mathrm{HF}} = 112$ dB for vertical radiation in this case. The relation of the pistons' dimensions to the fixed distance between adjacent piston centers that is also known as Active Radiating Factor (ARF) [14, Sec. 3.2], [21] amounts to approximately 0.82. For LF and MF the circular piston model is deployed, while for HF the line piston model is used. For the frequency band crossover, fourth-order Linkwitz-Riley filters with the transition frequencies $f_{\mathrm{LF,\ MF}} = 400$ Hz and $f_{\mathrm{MF,\ HF}} = 1500$ Hz are applied.

1.2 Venue Geometry

A multi-stand arena [10, Sec. 6.1] and an open-air amphitheater [18, Sec. 4.2.2] with audience and non-audience sections, i.e., zones to be covered and zones to be avoided, are modeled by two dimensional slice representations. The multi-stand arena slice representation consists of four audience lines with different tilt angles and typifies a rather complex source-receiver configuration. Venue 2 resembles the Waldbuehne in Berlin and is composed of two audience lines with different tilt angles for the sake of simplicity. It conforms to an extreme long-throw application. In this article near-fills, side-fills and delayed arrays— that are

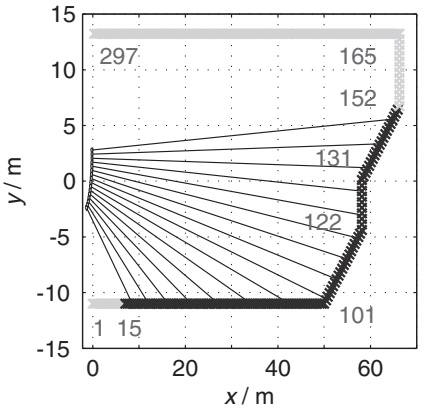

(a) Venue 1: multi-stand arena

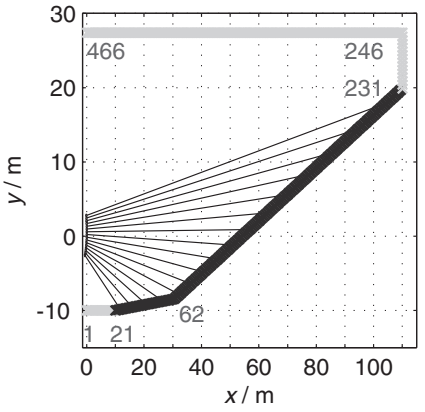

(b) Venue 2: amphitheater

Fig. 2. Venue slices within the *xy*-plane with audience (black) and non-audience/avoid (gray) zones and selected index numbers (change of audience/avoid zone and/or polygonal line's section angle) from M receiver positions.

routine in practical realizations—are not considered. Only the *xy*-plane is considered for vertical radiation, cf., Fig. 2. This is a common approach for optimization schemes of the loudspeakers' driving functions as the horizontal radiation is assumed to be convenient anyway, cf., [6–13].

The number of receiver positions taken into account is $M_{\mathrm{v1}} = 297$ for venue 1 and $M_{\mathrm{v2}} = 466$ for venue 2. They each comprise the receiver positions m with $m = 1, 2, ..., M$. This corresponds to a distance of 0.5 m between the receiver positions. The receiver positions are composed of M_{a} audience positions from the set $\mathcal{M}_{\mathrm{a}}$ and M_{na} non-audience positions from the set $\mathcal{M}_{\mathrm{na}}$ with $M = M_{\mathrm{a}} + M_{\mathrm{na}}$. They are characterized by the position vectors $\mathbf{x_m} = (x_m, y_m, 0)^{\mathrm{T}}$ and are numbered counterclockwise starting from the position under the LSA that is closest to the LSA (index 1, cf., Fig. 2). The venue slice coordinates are documented in Table 7 for venue 1 and in Table 8 for venue 2 in the Appendix.

Note that the terms *bright zone* and *dark zone* used in the field of multi-zone sound field synthesis (MZSFS) [22–24] correspond to the audience zone and the non-audience zone used in the field of sound reinforcement.

2 CALCULATION MODEL

The calculation model presented in this section is used for sound field prediction and for the evaluation of the different curving schemes. However, please note that the introduced analytical approach for finding LSA cabinet tilt angles (PALC) does not depend on a specific sound field prediction model.

Modeling multi-way cabinets, the total sound pressure at the receiver position m at the angular frequency ω is composed of the complex sound pressures, i.e., magnitudes and phases, of the different frequency bands as

$$P(m, \omega) = P_{\mathrm{LF}}(m, \omega) + P_{\mathrm{MF}}(m, \omega) + P_{\mathrm{HF}}(m, \omega). \quad (1)$$

Since the calculations are performed separately for each frequency band with a subsequent summation, the frequency band indices (LF, MF, HF) are omitted for generalization in the article. The sound field prediction is based on a complex-directivity point source (CDPS) model of baffled piston far-field radiation patterns. Its fundamental equation [16, Eq. (5)], [6, Eqs. (3–5)], [17, Sec. 1.1], [15, Eq. (11)] reads

$$P(m, \omega) = \sum_{i=1}^{i=V\,N} G(m, i, \omega)\, D(i, \omega) \quad (2)$$

considering the sources i with a total of N LSA cabinets each equipped with V loudspeakers in a specified frequency band.

$P(m, \omega)$ denotes the sound pressure at the receiver position $\mathbf{x_m}$ at the angular frequency ω. $G(m, i, \omega)$ terms the acoustic transfer function (ATF) from the i-th source to the m-th receiver position. The complex driving function $D(i, \omega)$ of the i-th source at the angular frequency ω is directly proportional to the source's velocity spectrum. Utilizing Eq. (2) for the sound field prediction, the calculated sound fields result from the superposition of the impact of each individual source i. The impact of each source is characterized by the source-receiver propagation characteristics—described by the ATF $G(m, i, \omega)$—and by the signal characteristics, i.e., the signal input as well as the electronic filters affecting the input of each source—described by the driving function $D(i, \omega)$.

Eq. (2) is modified including a loudspeaker sensitivity standardization in order to obtain absolute SPLs. Therefore $G(m, i, \omega)$ is considered as a scaled ATF for unit transformation

$$G(m, i, \omega) = p_0\, 10^{\frac{S(i,\omega)}{20}}\, R(\beta(m, i), \omega) \frac{\mathrm{e}^{-\mathrm{j}\,\frac{\omega}{c}\,|\mathbf{x_m} - \mathbf{x_{0,i}}|}}{|\mathbf{x_m} - \mathbf{x_{0,i}}|} \quad (3)$$

with the distance $|\mathbf{x_m} - \mathbf{x_{0,i}}|$ in meter, the reference sound pressure p_0 in Pascal and the sensitivity $S(i, \omega)$ in $\mathrm{dB_{SPL}}$ at 1 meter per Watt. The scaled ATF is composed of a specific far-field radiation pattern $R(\beta(m, i), \omega)$ for the radiation angle $\beta(m, i)$ at the angular frequency ω, the ideal point source wave propagation $\frac{\mathrm{e}^{-\mathrm{j}\,\frac{\omega}{c}\,|\mathbf{x_m} - \mathbf{x_{0,i}}|}}{|\mathbf{x_m} - \mathbf{x_{0,i}}|}$ with the velocity of sound c, the reference sound pressure p_0 that commonly amounts to $2 \cdot 10^{-5}$ Pa in air and the loudspeaker sensitivity $S(i, \omega)$ specifying the SPL in 1 m distance for 1 W electrical

input power. For all drivers and all frequencies per frequency band, the sensitivity is assumed to be constant, i.e., $S(i, \omega) = \text{const.}$

The complex driving function $D(i, \omega)$ of the i-th source at the angular frequency ω consists of the signal input $D_{\text{in}}(i, \omega)$, the complex optimized filter $D_{\text{opt}}(i, \omega)$ and the complex frequency band crossover as well as high-/lowpass filter $D_{\text{xo}}(\omega)$, thus

$$D(i, \omega) = D_{\text{in}}(i, \omega)\, D_{\text{opt}}(i, \omega)\, D_{\text{xo}}(\omega). \tag{4}$$

Gain and delay are mathematically considered as the amplitude and phase of these complex functions. As this article is exclusively focused on the curving of the LSA cabinets, only uniformly driven sources are considered, i.e.,

$$D_{\text{opt}}(i, \omega) = 1 \qquad \forall i \text{ and } \forall \omega. \tag{5}$$

The far-field radiation pattern of the baffled circular piston with radius Θ with a constant surface velocity is the normalized so-called jinc function [25, Eq. (26.42)]

$$R_{\text{c}}(\beta, \omega) = \frac{2\, J_1\left(\frac{\omega}{c}\Theta \sin\beta\right)}{\frac{\omega}{c}\Theta \sin\beta}, \tag{6}$$

denoting the cylindrical Bessel function of first kind of first order as $J_1(\,\cdot\,)$ [26, Eq. (10.2.2)]. The line piston models an ideal waveguide of height Λ_y for the HF band and its sinc-function far-field radiation pattern can be written as [25, Eq. (26.44)]

$$R_{\text{l}}(\beta, \omega) = \frac{\sin\left(\frac{\omega}{c}\frac{\Lambda_y}{2}\sin\beta\right)}{\frac{\omega}{c}\frac{\Lambda_y}{2}\sin\beta}. \tag{7}$$

Note that these patterns exhibit main lobe unity gain (i.e., 0 dB for $\beta = 0$) in order to control the energy radiated by the pistons via the assumed sensitivities.

Accounting for all receiver positions M for a single angular frequency ω, Eq. (2) is rewritten in matrix notation,

$$\mathbf{p}(\omega) = \mathbf{G}(\omega)\, \mathbf{d}(\omega) \tag{8}$$

with $\mathbf{p}(\omega)$ denoting the $(M \times 1)$ vector of sound pressures for all considered receiver positions $\mathbf{x_m}$, $\mathbf{G}(\omega)$ denoting the $(M \times VN)$ scaled ATF matrix for all sources i and for all receiver positions m and $\mathbf{d}(\omega)$ denoting the $(VN \times 1)$ vector of the complex driving functions for all sources i per angular frequency ω.

In line with this modeling, air absorption is neglected, a constant velocity of sound ($c = 343\,\text{m/s}$) and for the modeled sources infinite, straight baffles and a constant piston's surface velocity are assumed. The sound field predictions are performed for a logarithmically spaced frequency vector with $f_{\text{start}} = 200\,\text{Hz}$, $f_{\text{stop}} = 20\,\text{kHz}$ and 1/36 octave resolution.

3 CURVING OPTIMIZATION

Since it is a common approach to restrict the optimization schemes for the LSA driving functions to the vertical plane, it may also be advantageous to seek appropriate tilt angles of the LSA cabinets based on the venue slices from Sec. 1.2. In [8, 10, 13] this is executed by a numerical multi-objective optimization method that is used for determining the electronic drive as well. From [14, p. 929] the Wavefront Sculpture Technology (WST) criteria for LSAs are known. The practical consequences of criterion number four for determining the tilt angles are revisited in Sec. 3.1.

In Sec. 3.2 and Sec. 3.3 of this contribution, a purely analytical approach for finding practical LSA cabinet tilt angles with respect to the geometry of the receiver area and the intended coverage is presented: the polygonal audience line curving (PALC). PALC was originally developed to be applied beforehand to a numerical optimization of the loudspeakers' driving functions. The method can be used with different objectives, such as a constant interaction between adjacent cabinets with respect to the receiver geometry or by additionally considering SPL loss over distance.

3.1 Wavefront Sculpture Technology Approach

In [14, 27, 28], several criteria based on the Fresnel approach and analytical derivations of the diffraction theory are denoted as Wavefront Sculpture Technology. WST consists of five criteria how to create a homogeneous wavefront based on geometric LSA shaping. These criteria include the spatial sampling condition specifying the maximum allowed distance between adjacent sources and the Active Radiating Factor (ARF) theorem specifying the maximum relation of the pistons' dimensions to the fixed distance between the acoustic centers of adjacent sources. A further criterion defines the maximum allowed wavefront curvature at the waveguide's exit for high frequency radiation. These criteria are aimed for minimized grating lobe radiation that generally enables homogeneous wavefront shaping. The remaining criteria define the maximum allowed splay angle between adjacent LSA cabinets and an optimal array curvature to provide a homogeneous and frequency independent SPL loss over the audience using an appropriate wavefront shape, cf., [21, 29, 30].

Considering the splay angles, criterion number four states that the product of the splay angle α_n, i.e., the difference of the tilt angles of the $(n + 1)$-th and the n-th LSA cabinet, and the distance Δ_n from the center of the respective boxes to the receivers should be constant for an SPL attenuation of 3 dB per distance doubling.

Three different LSA curvatures derived from WST number four are introduced in [31]: the constant curvature, the J-shape curvature, and the progressive curvature as visualized in Fig. 3. The progressive curvature corresponds to the SPL attenuation of 3 dB per distance doubling directly resulting from WST number four. For an SPL attenuation of 6 dB per distance doubling the constant curvature with $\alpha_n = \text{const.}$ is recommended. If a constant sound pressure level over the audience zone is demanded, the J-shape curvature with $\alpha_n \cdot \Delta_n^2 = \text{const.}$ is used.

3.2 Polygonal Audience Line

The positions of the audience zones in the vertical radiation plane can be mathematically interpreted as polygonal line with the total length Γ_0. Fig. 4 represents an exemplary

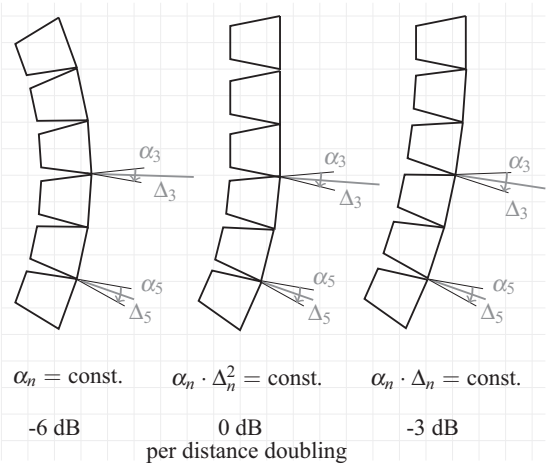

Fig. 3. Constant curvature, J-shape curvature, and progressive curvature according to WST for obtaining the denoted target SPL characteristics per distance doubling. The prerequisites for the splay angles α_n and the distances Δ_n to the receivers are denoted.

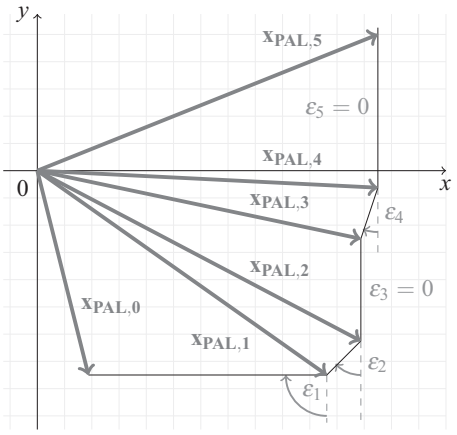

Fig. 4. Polygonal audience line (PAL) with K sections (in this case: $K = 5$). The start position of the k-th line section is specified by the vector $\mathbf{x}_{\mathbf{PAL},\mathbf{k-1}}$ and the stop position is given by the vector $\mathbf{x}_{\mathbf{PAL},\mathbf{k}}$. ε_k denotes the tilt angle of the k-th line section.

polygonal audience line (PAL) that is similar to venue 1 with K sections [$k = 0, 1, 2, ..., K$] with the tilt angles ε_k. The k-th line section is specified by the vectors $\mathbf{x}_{\mathbf{PAL},\mathbf{k-1}}$ for the start position and $\mathbf{x}_{\mathbf{PAL},\mathbf{k}}$ for the stop position. With these vectors, the total PAL length is

$$\Gamma_0 = \sum_{k=1}^{k=K} |\mathbf{x}_{\mathbf{PAL},\mathbf{k}} - \mathbf{x}_{\mathbf{PAL},\mathbf{k-1}}|. \tag{9}$$

The K PAL sections are covered by N LSA cabinets with $n = 1, 2, ..., N$. The polygonal audience line is therefore divided into N segments that represent the main radiation area of the LSA cabinets. Γ_n denotes the length of the n-th segment with the distance $\Gamma_{n,1}$ from the top to the center

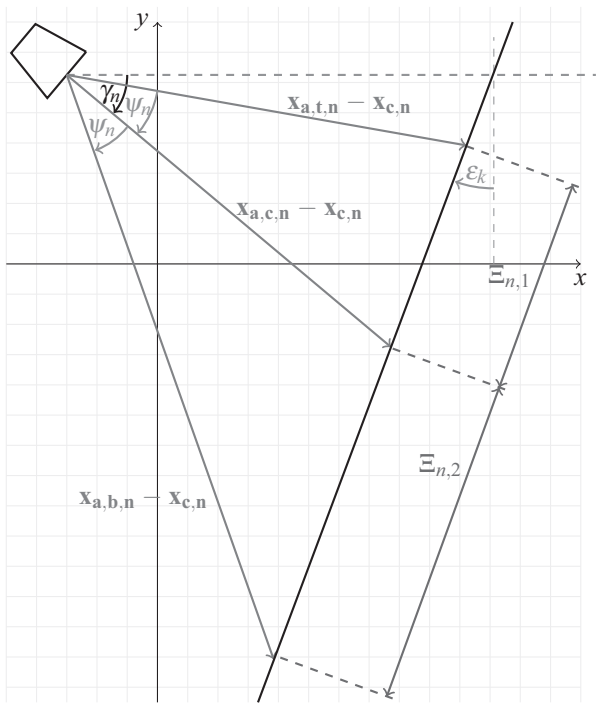

Fig. 5. Sketch of one section of the polygonal audience line with the n-th segment including only one section. The line section is not changed.

position and $\Gamma_{n,2}$ from the center to the bottom position of the segment, i.e., $\Gamma_n = \Gamma_{n,1} + \Gamma_{n,2}$. From

$$\Gamma = \sum_{n=1}^{n=N} \Gamma_n \tag{10}$$

the total length Γ of the covered audience line sections can be concluded. The different audience zones are indexed from the lowest to the highest audience positions. In order to calculate the position and the tilt angle γ_n of each LSA cabinet, it is necessary to start with the uppermost cabinet and compute iteratively from top to bottom.

3.3 PALC Algorithm

Starting with $n = 1$ and $k = K$, i.e., the topmost LSA cabinet and the topmost audience positions, n is iteratively increased and k is decreased. See Fig. 5 for detailed geometric information. Either the coverage angles ψ_n of all LSA cabinets are specified resulting in N required LSA cabinets that may differ from the intended original number of cabinets or the number N of LSA cabinets is fixed. The latter means that the angles ψ_n are found iteratively depending on the length Γ of the polygonal audience line and starting from the initial coverage angles ψ_{init} for all LSA boxes. Note that only discrete values can be typically set for the tilt angles of practical LSAs. By rounding the tilt angles γ_n in Eq. (11) after each calculation, the algorithm can be easily adapted concerning this matter. The algorithm is designed as follows:

I) Compute the tilt angle γ_n of the n-th LSA cabinet from the slope

$$\tan(-\gamma_n + \psi_n) = \frac{y_{\mathrm{a,t},n} - y_{\mathrm{c},n}}{x_{\mathrm{a,t},n} - x_{\mathrm{c},n}} \tag{11}$$

with the vector $\mathbf{x_{a,t,n}} = (x_{\mathrm{a,t},n},\, y_{\mathrm{a,t},n})^{\mathrm{T}}$ of the top position of the n-th polygonal audience line segment. The vector $\mathbf{x_{c,n}}$ of the n-th LSA cabinet center position is given as

$$\mathbf{x_{c,n}} = \begin{pmatrix} x_{\mathrm{c},n} \\ y_{\mathrm{c},n} \end{pmatrix} = \begin{pmatrix} x_{\mathrm{t},n} \\ y_{\mathrm{t},n} \end{pmatrix} - \frac{\Lambda_{y,\mathrm{LSA}}}{2} \begin{pmatrix} \sin\gamma_n \\ \cos\gamma_n \end{pmatrix} \tag{12}$$

with the height $\Lambda_{y,\mathrm{LSA}}$ of a single LSA cabinet and the vector $\mathbf{x_{t,n}} = (x_{\mathrm{t},n},\, y_{\mathrm{t},n})^{\mathrm{T}}$ of the n-th LSA cabinet top position. The initial values are set to

$$\begin{pmatrix} x_{\mathrm{t},1} \\ y_{\mathrm{t},1} \end{pmatrix} = \begin{pmatrix} x_{\mathrm{H}} \\ y_{\mathrm{H}} \end{pmatrix} \tag{13}$$

and

$$\mathbf{x_{a,t,1}} = \mathbf{x_{PAL,K}}. \tag{14}$$

x_{H} and y_{H} are the coordinates of the top position of the uppermost LSA cabinet and the vector $\mathbf{x_{PAL,K}}$ points at the top position of the K-th polygonal audience line section.

II) Calculate the center position vector $\mathbf{x_{c,n}}$ of every LSA cabinet with Eq. (12), i.e., for $n = 1, 2, ..., N$.

III) Compute the required distance $\Xi_{n,1}$ from the top to the center position of the n-th polygonal audience line segment with

$$\Xi_{n,1} = |\mathbf{x_{a,t,n}} - \mathbf{x_{c,n}}| \frac{\sin\psi_n}{\cos(\varepsilon_k - \gamma_n)}. \tag{15}$$

including the n-th coverage angle ψ_n and the tilt angle ε_k of the k-th polygonal audience line section.

We have to consider two cases: for case (i) equation

$$\Xi_{n,1} \leq |\mathbf{x_{a,t,n}} - \mathbf{x_{PAL,k-1}}| \tag{16}$$

holds, i.e., the calculated distance $\Xi_{n,1}$ is equal or smaller than the distance from the start position of the k-th polygonal audience line section to the top position of the n-th polygonal audience line segment, so that the section of the polygonal audience line is not changed. The center position vector of the current polygonal audience line segment can be calculated with

$$\mathbf{x_{a,c,n}} = \mathbf{x_{a,t,n}} + \Xi_{n,1} \begin{pmatrix} \cos\varepsilon_k \\ \sin\varepsilon_k \end{pmatrix} \tag{17}$$

and hence the segment's upper partial length $\Gamma_{n,1}$ is

$$\Gamma_{n,1} = \Xi_{n,1}. \tag{18}$$

If for case (ii) equation

$$\Xi_{n,1} > |\mathbf{x_{a,t,n}} - \mathbf{x_{PAL,k-1}}| \tag{19}$$

holds, i.e., the calculated distance $\Xi_{n,1}$ is greater than the distance from the start position of the k-th polygonal audience line section to the top position of the n-th polygonal audience line segment, so that the section of the polygonal audience line is changed. The n-th partial segment angle $\tilde{\psi}_n$ has to be calculated with

$$\frac{|\mathbf{x_{a,t,n}} - \mathbf{x_{PAL,k-1}}|}{|\mathbf{x_{a,t,n}} - \mathbf{x_{c,n}}|} = \frac{\sin(\psi_n - \tilde{\psi}_n)}{\cos(\varepsilon_k - \gamma_n + \tilde{\psi}_n)}. \tag{20}$$

The partial distance $\tilde{\Xi}_{n,1}$ from the top to the center position of the n-th polygonal audience line segment is thus

$$\tilde{\Xi}_{n,1} = |\mathbf{x_{PAL,k-1}} - \mathbf{x_{c,n}}| \frac{\sin\tilde{\psi}_n}{\cos(\varepsilon_{k-1} - \gamma_n)} \tag{21}$$

and the center position vector of the current polygonal audience line segment can be written as

$$\mathbf{x_{a,c,n}} = \mathbf{x_{PAL,k-1}} + \tilde{\Xi}_{n,1} \begin{pmatrix} \cos\varepsilon_{k-1} \\ \sin\varepsilon_{k-1} \end{pmatrix} \tag{22}$$

and hence

$$\Gamma_{n,1} = |\mathbf{x_{a,t,n}} - \mathbf{x_{PAL,k-1}}| + \tilde{\Xi}_{n,1} \tag{23}$$

is the segment's upper partial length.

IV) Update k: k is not changed if the section of the polygonal audience line was not changed (step III, case (i)). k has to be decreased by 1 if the section of the polygonal audience line was changed (step III, case (ii)).

V) Calculate the required distance $\Xi_{n,2}$ from the center to the bottom position of the n-th polygonal audience line segment with

$$\Xi_{n,2} = |\mathbf{x_{a,c,n}} - \mathbf{x_{c,n}}| \frac{\sin\psi_n}{\cos(\varepsilon_k - \gamma_n - \psi_n)} \tag{24}$$

including the n-th coverage angle ψ_n and the tilt angle ε_k of the k-th polygonal audience line section.

We again have to consider two cases: for case (i) equation

$$\Xi_{n,2} > |\mathbf{x_{a,c,n}} - \mathbf{x_{PAL,k-1}}| \tag{25}$$

holds, i.e., the calculated distance $\Xi_{n,2}$ is greater than the distance from the start position of the k-th polygonal audience line section to the center position of the n-th polygonal audience line segment, so that the section of the polygonal audience line is changed. The n-th partial segment angle $\tilde{\psi}_n$ then has to be calculated with

$$\frac{|\mathbf{x_{a,c,n}} - \mathbf{x_{PAL,k-1}}|}{|\mathbf{x_{a,c,n}} - \mathbf{x_{c,n}}|} = \frac{\sin\tilde{\psi}_n}{\cos(\varepsilon_k - \gamma_n - \tilde{\psi}_n)}. \tag{26}$$

Therefore, the partial distance $\tilde{\Xi}_{n,2}$ from the center to the bottom position of the n-th polygonal audience line segment is

$$\tilde{\Xi}_{n,2} = |\mathbf{x_{PAL,k-1}} - \mathbf{x_{c,n}}| \frac{\sin(\psi_n - \tilde{\psi}_n)}{\cos(\varepsilon_{k-1} - \gamma_n - \psi_n)} \tag{27}$$

and the bottom position vector of the current polygonal audience line segment can be written as

$$\mathbf{x_{a,b,n}} = \mathbf{x_{PAL,k-1}} + \tilde{\Xi}_{n,2} \begin{pmatrix} \cos\varepsilon_{k-1} \\ \sin\varepsilon_{k-1} \end{pmatrix}. \tag{28}$$

Hence the segment's lower partial length is

$$\Gamma_{n,2} = |\mathbf{x_{a,c,n}} - \mathbf{x_{PAL,k-1}}| + \tilde{\Xi}_{n,2}. \tag{29}$$

If for case (ii) equation

$$\Xi_{n,2} \leq |\mathbf{x_{a,c,n}} - \mathbf{x_{PAL,k-1}}| \tag{30}$$

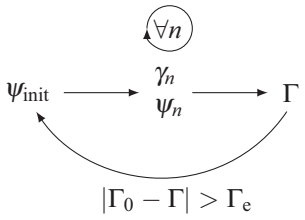

Fig. 6. Overview of the iterative PALC process with the initial coverage angle ψ_{init}, the n-th coverage angle ψ_n, the tilt angle γ_n of the n-th LSA cabinet, the total polygonal audience line length Γ_0, the total length of the covered polygonal audience line sections Γ and the termination condition Γ_e.

is valid, i.e., the calculated distance $\Xi_{n,2}$ is equal or smaller than the distance from the start position of the k-th polygonal audience line section to the center position of the n-th polygonal audience line segment, so that the section of the polygonal audience line is not changed, the bottom position vector of the current polygonal audience line segment can be calculated with

$$\mathbf{x_{a,b,n}} = \mathbf{x_{a,c,n}} + \Xi_{n,2}\begin{pmatrix}\cos\varepsilon_k \\ \sin\varepsilon_k\end{pmatrix} \tag{31}$$

and eventually

$$\Gamma_{n,2} = \Xi_{n,2}. \tag{32}$$

is the segment's lower partial length.

VI) Update k: k is not changed if the section of the polygonal audience line was not changed (step V, case (ii)). k has to be decreased by 1 if the section of the polygonal audience line was changed (step V, case (i)).

The steps I) – VI) have to be repeated until $n = N$ and $k = 0$. If the number N of LSA cabinets is fixed and the coverage angles ψ_n are to be determined, the values of the total polygonal audience line length Γ_0 and of the total length of the covered polygonal audience line sections Γ are compared after each complete iteration. All ψ_n are decreased if the total length of the covered polygonal audience line sections Γ is greater than the total polygonal audience line length Γ_0, and all ψ_n are increased if Γ is smaller than Γ_0. This termination condition is denoted as Γ_e. In Fig. 6, the iteration process is visualized.

4 EVALUATION

Acoustic simulations based on the CDPS model including far-field radiation patterns of baffled line and circular pistons provide the data for an evaluation of the introduced approach. The evaluation is performed for two conditions and in comparison with typical standard LSA curving schemes such as straight, arc, J, and progressive [30] as well as two numerically optimized versions resulting from the Martin Audio Display prediction and optimization software [8, 13]. Note that we deliberately distinguish between the WST curvatures from Sec. 3.1 and the specifications in [30]. The nomenclature from the latter is used for the curvings in this article.

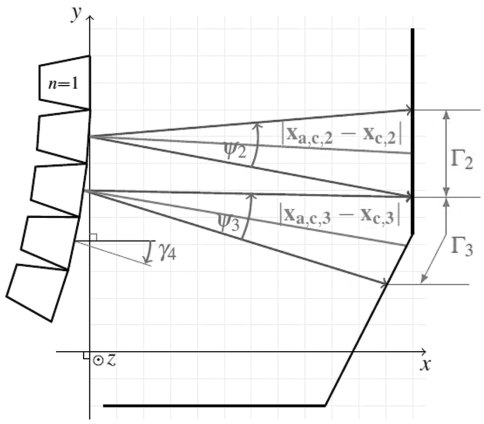

Fig. 7. Sketch of the LSA setup following the PALC1 and PALC2 approach. It is exemplarily shown for the second and the third LSA box. γ_n denotes the tilt angle of the n-th LSA cabinet, ψ_n denotes the n-th coverage angle, $|\mathbf{x_{a,c,n}} - \mathbf{x_{c,n}}|$ denotes the distance from the center positions of the n-th polygonal audience line segment and of the n-th LSA cabinet and Γ_n denotes the length of the n-th polygonal audience line segment.

PALC1 incorporates the goal of an invariant interaction between adjacent cabinets with respect to the receiver geometry in order that the radiated sound of the different sources overlap at a constant coverage angle ψ in the far-field of the individual sources. This constraint simply reads

$$\text{PALC1:} \qquad \psi_1 = \psi_2 = \psi_3 = ... = \text{const.} \tag{33}$$

PALC1 is similar to an arc array but the goal does not refer to the array itself, i.e., constant splay angles between all cabinets, but it refers to the shape of the receiver geometry.

The distances of the different positions from the sources and the desired sound field are considered in PALC2. It demands a constant product of the coverage angle ψ and the distance from the source to the receiver positions, i.e., the distance from the center positions of the n-th polygonal audience line segment and of the n-th LSA cabinet,

$$\begin{aligned}\text{PALC2:} \qquad & \psi_1 \cdot |\mathbf{x_{a,c,1}} - \mathbf{x_{c,1}}| \\ & = \psi_2 \cdot |\mathbf{x_{a,c,2}} - \mathbf{x_{c,2}}| = \ldots = \text{const.},\end{aligned} \tag{34}$$

cf., Fig. 5. This results from an approximation of

$$\begin{aligned}&\tan\psi_1 \cdot |\mathbf{x_{a,c,1}} - \mathbf{x_{c,1}}| \\ &\quad = \tan\psi_2 \cdot |\mathbf{x_{a,c,2}} - \mathbf{x_{c,2}}| = \ldots = \text{const.}\end{aligned} \tag{35}$$

for small ψ_n. Eq. (35) arises from a simplification of attaining a constant length Γ_n for all n polygonal audience line segments. In Fig. 7 the geometric variables being relevant for PALC1 and PALC2 are exemplarily shown for the second and the third LSA box. The PALC2 constraint should not be confused with the Wavefront Sculpture Technology criterion number four, cf., Sec. 3.1, Table 9, and Table 10.

For the evaluation cases MA1 and MA2, the tilt angles were extracted from the commercially available prediction and optimization software Martin Audio Display (version 2.1.10) that provides suitable tilt angles and also—if desired—the electronic control by means of a numerical multi-objective optimization scheme [8, 10, 13]. The

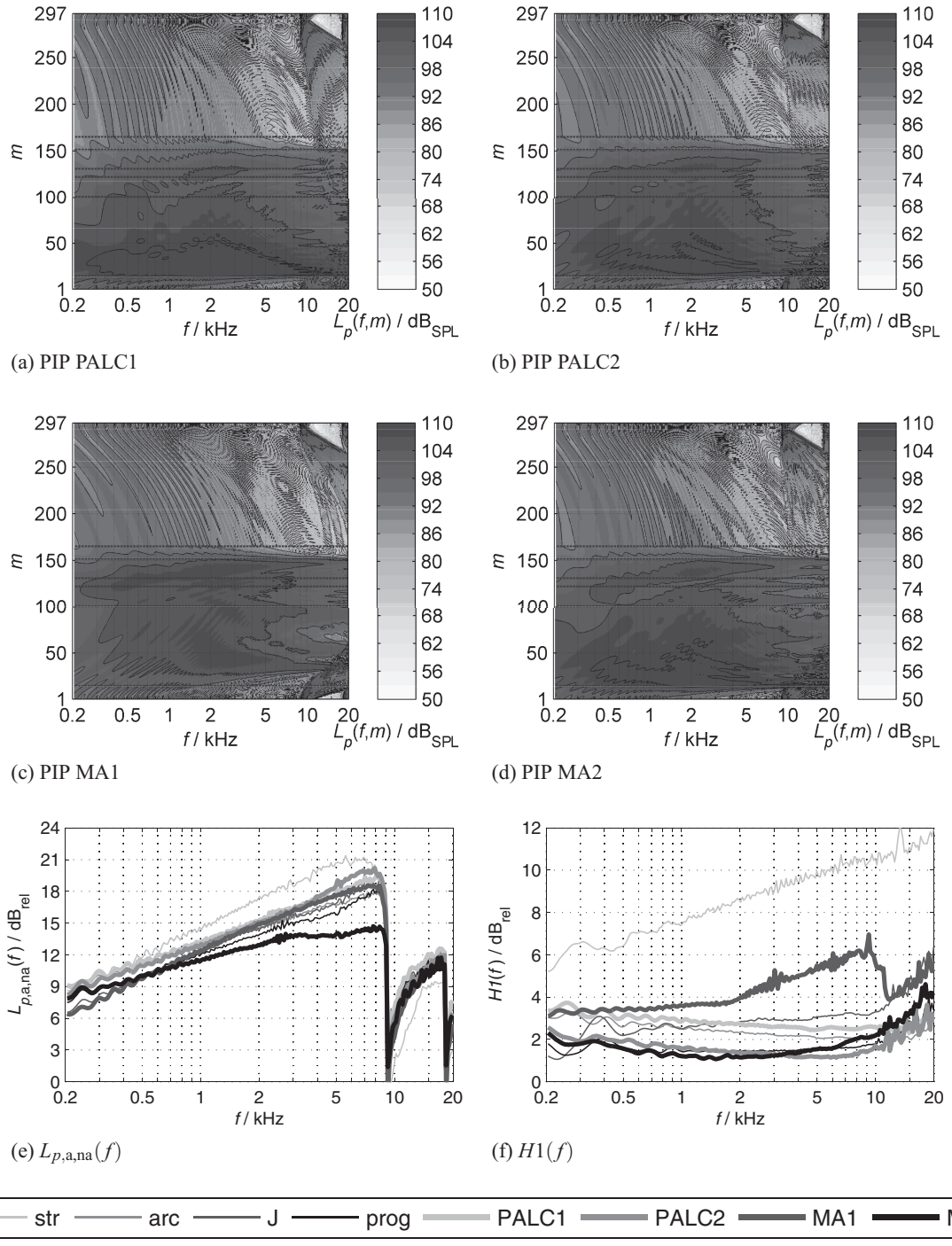

(a) PIP PALC1 (b) PIP PALC2

(c) PIP MA1 (d) PIP MA2

(e) $L_{p,\mathrm{a,na}}(f)$ (f) $H1(f)$

Fig. 8. Position index plots (PIPs) depending on the frequency f and the position index m for PALC1, PALC2, MA1 and MA2, the acoustic contrast $L_{p,\mathrm{a,na}}(f)$ and the homogeneity measure $H1(f)$ depending on the frequency f for all analyzed curvings for venue 1 from Fig. 2a. The dashed horizontal lines in the PIPs refer to the selected index numbers in Fig. 2a which represent changes of the audience/avoid zone and/or of the polygonal line's section angle.

weighting parameters for target and leakage each are set to 1 for MA1 and are set to 10 and 4 for MA 2 allowing a SPL attenuation of 10 dB from the first to the last audience position. Note that the optimization parameters target and leakage are quantitatively specified as the absolute error Eq. (36) and the acoustic contrast Eq. (39) in our case.

A reasonable selection of the evaluation criteria that were suggested in [20] is utilized to assess the quality of the different curving approaches. The position index plots (PIPs) show the resulting SPL spectra at all receiver positions $\mathbf{x_m}$, i.e., the sound pressure levels $L_p(\omega, m)$ depending on the angular frequency ω and the position index m. They are depicted in Fig. 8 for PALC1, PALC2, MA1, and MA2 for venue 1 and in Fig. 9 for venue 2. Also known as positional map, the PIPs were used in [7, 8, 10, 11, 13] as well. The "ideal" PIP depends on the application. In general, it is

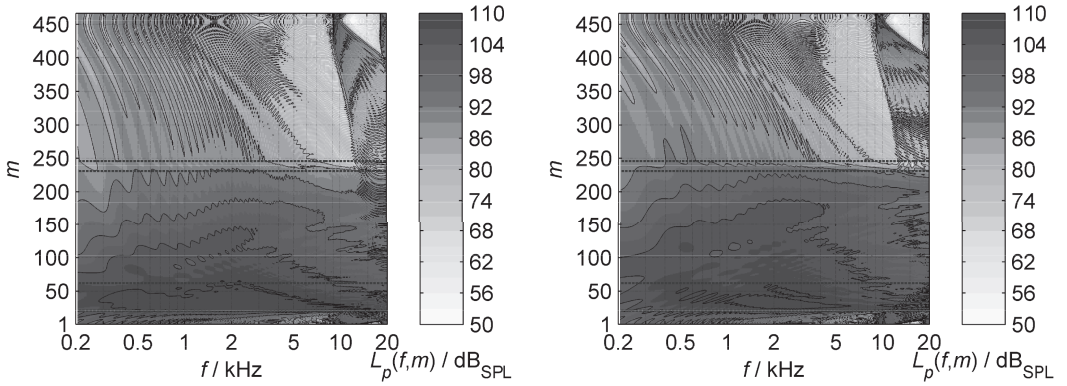

(a) PIP PALC1 (b) PIP PALC2

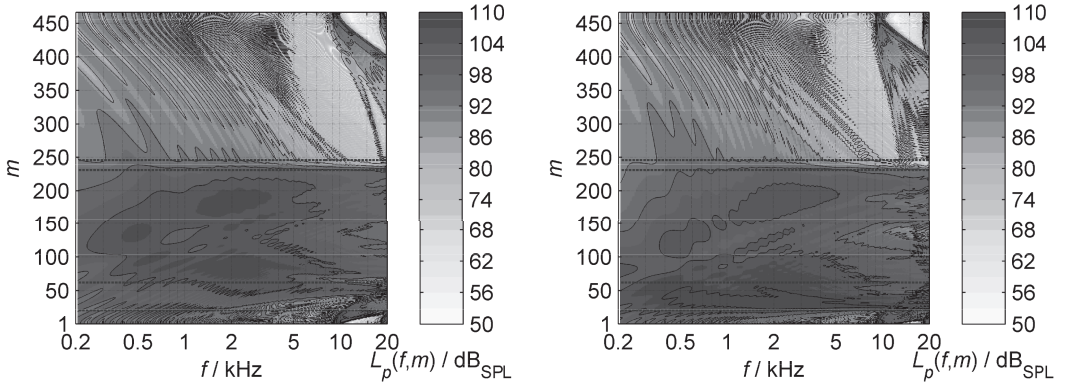

(c) PIP MA1 (d) PIP MA2

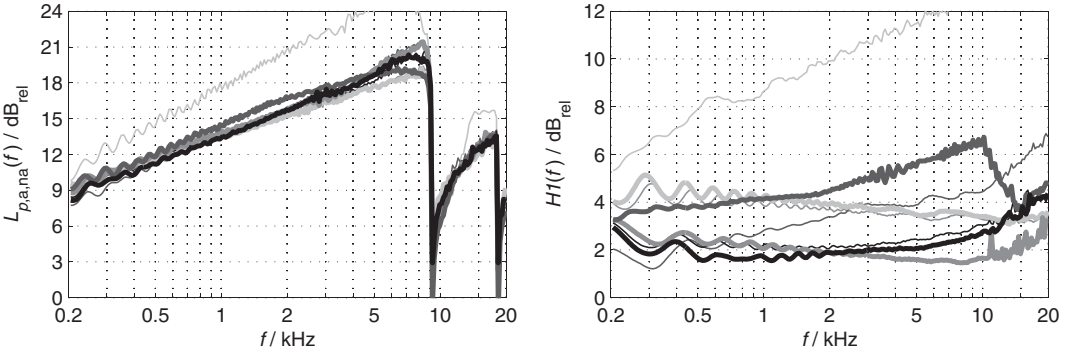

(e) $L_{p,\mathrm{a,na}}(f)$ (f) $H1(f)$

Fig. 9. Position index plots (PIPs) depending on the frequency f and the position index m for PALC1, PALC2, MA1 and MA2, the acoustic contrast $L_{p,\mathrm{a,na}}(f)$ and the homogeneity measure $H1(f)$ depending on the frequency f for all analyzed curvings for venue 2 from Fig. 2b. The dashed horizontal lines in the PIPs refer to the selected index numbers in Fig. 2b which represent changes of the audience/avoid zone and/or of the polygonal line's section angle.

desired that only little energy is radiated into the non-audience zones compared to the audience zones, i.e., for the position indices m that belong to the non-audience zones, low SPLs are expected all frequencies f. For the receiver positions m that belong to the audience zones, maximum SPLs, a predefined SPL or a constant SPL at all frequencies may be desired.

The quantitative evaluation is based on three technical quality measures. Denoting the squared Euclidean norm $\|\cdot\|_2^2$ [26, Eq. (3.2.13)], the frequency dependent absolute amplitude error [20, Eq. (16)]

$$E(\omega) = \left\| \underset{m\in\mathcal{M}_\mathrm{a}}{\mathbf{p}(\omega)} - \underset{m\in\mathcal{M}_\mathrm{a}}{\mathbf{p}_\mathrm{des}(\omega)} \right\|_2^2 \tag{36}$$

between the obtained sound field $\mathbf{p}(\omega)$ and the desired sound field $\mathbf{p}_\mathrm{des}(\omega)$ in the audience zone, i.e., $m \in \mathcal{M}_\mathrm{a}$, is additionally smoothed in third-octave bands. The desired

sound field $\mathbf{p}_{\mathrm{des}}(\omega)$ could in principle be set arbitrarily. However, the used array geometry restricts the choice to physically realizable wave fronts. Typically a desired level decay over the audience zone and a level offset for the avoid zone can be defined in practical realizations [8].

We have chosen

$$P_{\mathrm{des}}(m,\,\omega) \propto \frac{\mathrm{e}^{-\mathrm{j}\frac{\omega}{c}|\mathbf{x_m}-\mathbf{x_S}|}}{\sqrt{|\mathbf{x_m}-\mathbf{x_S}|}} \tag{37}$$

at the receiver position m and the angular frequency ω as the basis for the comparison. This desired sound field complies with a sound field generated by a virtual line source at the position $\mathbf{x_S}$ deploying the large argument-approximation of the 2D Green's function, i.e., for high frequencies and/or in the far-field [32, Eq. (26)]. The source position $\mathbf{x_S}$ is individually calculated for each LSA configuration depending on the top position vector $\mathbf{x_{t,1}}$ of the first (topmost) LSA cabinet and the bottom position vector $\mathbf{x_{b,16}}$ of the last (bottommost) LSA cabinet, i.e.,

$$\mathbf{x_S} = \frac{1}{2}\left[\begin{pmatrix} x_{\mathrm{t},1} \\ y_{\mathrm{t},1} \end{pmatrix} + \begin{pmatrix} x_{\mathrm{b},16} \\ y_{\mathrm{b},16} \end{pmatrix}\right]. \tag{38}$$

A target sound pressure level of 100 $\mathrm{dB_{SPL}}$ at the first receiver position within the audience zone is expected.

Alternatively, we could have also chosen other desired sound fields, such as constant SPLs or maximum SPLs at all receiver positions m or a 6 dB SPL loss per distance doubling. Since this article is focused on modeled loudspeaker data, we selected an ideal 3 dB SPL loss per distance doubling which is provided by an infinite, continuous line source and can be unambiguously expressed by Eq. (37). Using measured loudspeaker data, other target sound fields may be more advantageous, such as sound fields that are directly based on the sound fields generated by uniformly driven LSAs.

Moreover, the frequency dependent relation of the obtained average SPLs of the audience and the non-audience zone

$$L_{p,\mathrm{a,na}}(\omega) = 10\,\log_{10}\left(\frac{\frac{1}{M_{\mathrm{a}}}\left\|\mathbf{p}(\omega)_{m\in\mathcal{M}_{\mathrm{a}}}\right\|_2^2}{\frac{1}{M_{\mathrm{na}}}\left\|\mathbf{p}(\omega)_{m\in\mathcal{M}_{\mathrm{na}}}\right\|_2^2}\right) \tag{39}$$

[20, Eq. (18)] is evaluated, i.e., considering the sound pressures for the receiver positions of the set of the audience positions in the numerator and of the set of the non-audience positions in the denominator. This measure is depicted in Fig. 8e and Fig. 9e and corresponds to the acoustic contrast [22, Eq. (16)], [23, Eq. (2)] established in MZSFS. Quantifying the homogeneity of the generated sound field based on the magnitudes, neglecting the phases in this case, the frequency dependent standard deviation of the distance compensated SPLs of all audience positions

$$H1(\omega) = \underset{m\in\mathcal{M}_{\mathrm{a}}}{\sigma}\left[20\,\log_{10}\left(\frac{|P(m,\,\omega)|}{p_0}\sqrt{\frac{|\mathbf{x_m}-\mathbf{x_S}|}{|\mathbf{x_{min(m)}}-\mathbf{x_S}|}}\right)\right], \tag{40}$$

cf., [11, e.g. Fig. 6, Fig. 8], is analyzed. σ denotes the standard deviation and $\mathbf{x_{min(m)}}$ is the vector for the first audience position in this case. Note that the root term results from the distance compensation referring to the desired 3 dB SPL loss per distance doubling of a virtual line source. The homogeneity measure is visualized in Fig. 8f and Fig. 9f.

5 DISCUSSION

For two concert venues, the proposed algorithm for optimizing the tilt angles of line array cabinets was evaluated with respect to different quality measures. The position index plots (PIPs) for venue 1 (Fig. 2a) shown in Fig. 8 reveal that only little energy is radiated into the non-audience zones compared to the audience zones for all of the algorithmic curving schemes. Note that the dashed horizontal lines in the PIPs refer to the selected index numbers in Fig. 2 which represent changes of the audience/avoid zone and/or of the polygonal line's section angle. For both venues, the audience zone is located between the second uppermost and the bottommost dashed horizontal line.

The intended behavior is confirmed by $L_{p,\mathrm{a,na}}(\omega)$ from Eq. (39) in Fig. 8e for the optimized curvings as well as for the standard curving schemes (straight, arc, J, and progressive) that were manually adjusted to the receiver geometry. It can be seen in the PIPs and by means of $L_{p,\mathrm{a,na}}(\omega)$ that the relation of the energy radiated into the audience and the non-audience zones is very similar for all tilt angle sets and increases with increasing frequency. The latter results from the radiation characteristics of the sources: the radiation is more directed, the higher the frequency.

$L_{\,p,\mathrm{a,na}}(\omega)$ features acceptable values larger than 12 dB for frequencies above 1 kHz and below ca. 8.5 kHz. For frequencies above ca. 8.5 kHz spatial aliasing effects are visible leading to more energy in the non-audience zones and significantly reduced acoustic contrast values. The grating lobes that are causal for that appear at rather high frequencies compared to conventional LSA designs due to the small distances between the HF sources. Choosing equal weights for target and leakage, the final angle of the numerically optimized MA1 is rather small. Therefore, the first audience rows are hardly reinforced as it can be deduced from the MA1 PIP. Increasing the target weight in relation to the leakage weight, the final angle of MA2 approximately corresponds to those of the other curving methods. Comparing MA1 and MA2, the effect of the reduced focus on leakage can be clearly observed by means of $L_{p,\mathrm{a,na}}(\omega)$ for frequencies above ca. 700 Hz.

Significant performance differences can be found with the help of the homogeneity measure $H1(\omega)$ from Eq. (40). The straight array does not cover the whole audience zone so that there are large deviations considering the front, the middle, and the back audience positions. For the front positions, MA1 shows a similar performance due to the small final angle. The arc and J array suffer from limited adjustment capabilities to the given receiver geometry. PALC2 and MA2 provide the best homogeneity values with MA2

being more homogeneous than PALC2 for frequencies below ca. 2 kHz. For frequencies above ca. 2 kHz, $H1(\omega)$ of PALC2 is smaller than the one of MA2 for up to (1...1.5) dB. The PIP of MA2, however, reveals some coverage gaps for the middle positions around $m \approx 110$ due to some large splay angles. An invariant interaction between adjacent cabinets that was intended with PALC1 does not seem to be practical considering homogeneity. As expected, the progressive curving yields solid results without paying attention to the specific composition of the receiver geometry.

For venue 2 (Fig. 2b) resembling a typical open-air amphitheater, the results are very similar to those for venue 1. Only the expected difference of the acoustic contrast $L_{p,\mathrm{a,na}}(\omega)$ between MA1 and MA2 is not observable for venue 2. Note that the absolute error $E(\omega)$ from Eq. (36) is not visualized as it provides no meaningful results for the uniformly driven LSAs.

The tilt angles calculated with the PALC2 approach were compared with the established WST criterion number four for venue 1 and venue 2. It can be found in Table 9 and Table 10 in the Appendix that PALC2 provides results that are in accordance with the demand for a constant product of the splay angles and the respective source-to-receiver distances. The absolute values of the products are constant depending on the polygonal audience line section that the involved LSA cabinets are pointing at.

Using the PALC approach, it is assumed that all deployed LSA cabinets have similar radiation patterns. Frequency dependent behavior and individual characteristics of the LSA radiation are not considered. All audio frequencies are treated equally, there is no preference for selected frequencies or frequency bands. This enables a low-computational and straight-forward calculation without the need of numerical algorithms requiring high computational effort, but this may reduce the achievable accuracy. However, PALC completely incorporates the present receiver geometry. In addition, the comparison of the PALC2 results and the respective WST criterion reveals that the assumptions do not turn away from the assumptions made for the established WST approach.

The evaluation is not based on measurements in this article but only on simulations. Therefore, the results may differ from measured and perceived sound fields of practical LSAs. Since typical trial-and-error-approaches by sound engineers, i.e., manual adjustment of the LSA cabinet tilt angles, follow similar principles as PALC and due to the PALC tilt angles being in accordance with WST, similar results can be expected for measurements. The precision of the sound field prediction may be improved by incorporating data from balloon measurements that also include the influence of adjacent cabinets or by using boundary element method (BEM) data [17]. Measured loudspeaker data can be included as far-field radiation patterns $R(\beta, \omega)$ in the deployed CDPS calculation model. Comparing the sound fields generated with modeled and these measured loudspeaker data, we concluded that the design and development of optimization algorithms can be performed independent of the data [33]. Future verifications based on hands-on measurements are, however, essential.

6 CONCLUSION

Sound reinforcement in different venues requires adapted curving of line source arrays (LSAs). A purely analytical approach for finding appropriate LSA cabinet tilt angles was presented in this article. The polygonal audience line curving (PALC) is based on the geometry of the receiver area and the intended coverage. In comparison with typical standard LSA curving schemes, we conclude that the PALC is superior due to its flexible adaptability with respect to the receiver geometry.

This algorithm is faster than numerical methods. Since identical specifications for the presented analytical and the evaluated numerical optimization approach cannot be completely ensured, a final comparative statement regarding accuracy does not seem to be advisable. These specifications especially comprise the exact conversion from the selectable goal parameters to the desired sound field as well as the considered frequency ranges, possibly also weighted, of the numerical algorithms used as a reference and the fact that these are based on proprietary, not extractable loudspeaker directivity data. The effort and the computing time of the numerical approach are however significantly higher than for the analytical approach.

The PALC algorithm can be easily extended so that it only seeks from a discrete set of tilt angle values as it is required for practical realizations. It can be easily used in combination with subsequent electronic wavefront shaping. Since the LSA setup is restricted to fundamentals in this article, neglecting several aspects such as changes and uncertainties of the source configuration and of the frequency-dependent behavior, different LSA setups and their characteristics along with several curving optimization schemes should be discussed in the future. Also the human perception of phase effects in sound fields generated by LSAs should be examined. By listening tests, it may be possible to find quality criteria for phase position index plots (PIPs) analogue to the magnitude PIPs.

7 REFERENCES

[1] D. Scheirman, "Large-Scale Loudspeaker Arrays: Past, Present and Future (Part Two—Electroacoustic Considerations)," presented at the *AES 59th International Conference: Sound Reinforcement Engineering and Technology* (2015 July), conference paper 1-3.

[2] Martin Audio Ltd., "User Guide. Display 2.2, version 3.2," Tech. rep., https://martin-audio.com/downloads/software/Display-2.2-User-Guide-v3.2.pdf, last seen on 2017-08-21 (2017).

[3] Eastern Acoustic Works Inc., "EAW Resolution 2. Help File," Tech. rep., http://eaw.com/docs/3_Manuals/EAW last seen on 2017-08-21 (2017).

[4] d&b Audiotechnik GmbH, "ArrayCalc Simulation Software V8. ArrayProcessing Feature, Technical White Paper," Tech. rep., http://www.dbaudio.com/en/support/downloads/category/download/4195.html, last seen on 2017-08-21 (2017).

[5] AFMG Technologies GmbH, "AFMG FIRmaker. AFMG White Paper," Tech. rep., http://www.afmg-support.eu/SoftwareDownloadBase/FIRmaker/FIRmaker_White_Paper.pdf, last seen on 2017-08-21 (2017).

[6] G. W. van Beuningen and E. W. Start, "Optimizing Directivity Properties of DSP Controlled Loudspeaker Arrays," *Proc. of the Inst. of Acoustics: Reproduced Sound*, vol. 22, no. 6, pp. 17–37 (2000).

[7] A. Thompson, "Real World Line Array Optimisation," *Proc. of the Inst. of Acoustics*, vol. 30, no. 6 (2008).

[8] A. Thompson, "Improved Methods for Controlling Touring Loudspeaker Arrays," presented at the *127th Convention of the Audio Engineering Society* (2009 Oct.), convention paper 7828.

[9] M. Terrell and M. Sandler, "Optimising the Controls of a Homogenous Loudspeaker Array," presented at the *129th Convention of the Audio Engineering Society* (2010 Nov.) convention paper 8159.

[10] A. Thompson, J. Baird, and B. Webb, "Numerically Optimised Touring Loudspeaker Arrays - Practical Applications," presented at the *131st Convention of the Audio Engineering Society* (2011 Oct.), convention paper 8511.

[11] S. Feistel, M. Sempf, K. Köhler, and H. Schmalle, "Adapting Loudspeaker Array Radiation to the Venue Using Numerical Optimization of FIR Filters," presented at the *135th Convention of the Audio Engineering Society* (2013 Oct.), convention paper 8937.

[12] A. Thompson and J. Luzarraga, "Drive Granularity for Straight and Curved Loudspeaker Arrays," *Proc. of the Inst. of Acoustics*, vol. 35, no. 2, pp. 210–218 (2013).

[13] A. Thompson, "Line Array Splay Angle Optimisation," *Proc. of the Inst. of Acoustics*, vol. 28, no. 8, pp. 135–148 (2006).

[14] M. Urban, C. Heil, and P. Bauman, "Wavefront Sculpture Technology," *J. Audio Eng. Soc.*, vol. 51, pp. 912–932 (2003 Oct.).

[15] S. Feistel, A. Thompson and W. Ahnert, "Methods and Limitations of Line Source Simulation," *J. Audio Eng. Soc.*, vol. 57, pp. 379–402 (2009 Jun.).

[16] D. G. Meyer, "Computer Simulation of Loudspeaker Directivity," *J. Audio Eng. Soc.*, vol. 32, pp. 294–315 (1984 May).

[17] P. Meyer and R. Schwenke, "Comparison of the Directional Point Source Model and BEM Model for Arrayed Loudspeakers," *Proc. of the Inst. of Acoustics*, vol. 25, no. 4 (2003).

[18] F. Schultz, *Sound Field Synthesis for Line Source Array Applications in Large-Scale Sound Reinforcement*, Ph.D. thesis, University of Rostock (2016).

[19] F. Straube, F. Schultz, and S. Weinzierl, "On the Effect of Spatial Discretization of Curved Line Source Arrays," Fortschritte der Akustik: Tagungsband d. 41. DAGA, Nuremberg, pp. 459–462 (2015).

[20] F. Straube, F. Schultz, M. Makarski, S. Spors, and S. Weinzierl, "Evaluation Strategies for the Optimization of Line Source Arrays," presented at the *AES 59th International Conference: Sound Reinforcement Engineering and Technology* (2015 July), conference paper 2-1.

[21] F. Schultz, F. Straube, and S. Spors, "Discussion of the Wavefront Sculpture Technology Criteria for Straight Line Arrays," presented at the *138th Convention of the Audio Engineering Society* (2015 May), convention paper 9323.

[22] J.-W. Choi and Y.-H. Kim, "Generation of an Acoustically Bright Zone with an Illuminated Region Using Multiple Sources," *J. Acoust. Soc. Am.*, vol. 111, no. 4, pp. 1695–1700 (2002 Apr.), doi:https://doi.org/10.1121/1.1456926.

[23] P. Coleman, P. J. Jackson, M. Olik, M. Møller, M. Olsen, and J. A. Pedersen, "Acoustic Contrast, Planarity and Robustness of Sound Zone Methods Using a Circular Loudspeaker Array," *J. Acoust. Soc. Am.*, vol. 135, no. 4, pp. 1929–1940 (2014 Apr.), doi:https://doi.org/10.1121/1.4866442.

[24] M. R. Bai, J.-C. Wen, H. Hsu, Y.-H. Hua, and Y.-H. Hsieh, "Investigation on the Reproduction Performance versus Acoustic Contrast Control in Sound Field Synthesis," *J. Acoust. Soc. Am.*, vol. 136, no. 4, pp. 1591–1600 (2014 Oct.), doi:https://doi.org/10.1121/1.4894693.

[25] E. Skudrzyk, *The Foundations of Acoustics* (Springer, New York, 1971).

[26] F. W. J. Olver, D. W. Lozier, R. F. Boisvert, and C. W. Clark, *NIST Handbook of Mathematical Functions, 1st ed.* (Cambridge University Press, Cambridge, 2010).

[27] C. Heil and M. Urban, "Sound Fields Radiated by Multiple Sound Sources Arrays," presented at the *92nd Convention of the Audio Engineering Society* (1992 Mar.), convention paper 3269.

[28] M. Urban, C. Heil, and P. Bauman, "Wavefront Sculpture Technology," presented at the *111th Convention of the Audio Engineering Society* (2001 Nov.), convention paper 5488.

[29] M. S. Ureda, "Line Arrays: Theory and Applications," presented at the *110th Convention of the Audio Engineering Society* (2001 May), convention paper 5304.

[30] M. S. Ureda, "Analysis of Loudspeaker Line Arrays," *J. Audio Eng. Soc.*, vol. 52, pp. 467–495 (2004 May).

[31] L'Acoustics, "Training Module Variable Curvature Line Source" (2016).

[32] J. Ahrens and S. Spors, "Sound Field Reproduction Using Planar and Linear Arrays of Loudspeakers," *IEEE Trans. on Audio Speech Language Process.*, vol. 18, no. 8, pp. 2038–2050 (2010 Nov.).

[33] F. Straube, F. Schultz, M. Makarski, and S. Weinzierl, "Optimized Driving Functions for Curved Line Source Arrays Using Modeled and Measured Loudspeaker Data," *Fortschritte der Akustik: Tagungsband d. 42. DAGA, Aachen*, pp. 1136–1139 (2016).

APPENDIX

Table 2. List of variables—sound field prediction and evaluation

c	velocity of sound
$D(i, \omega)$	complex driving function of the i-th source at the angular frequency ω
$\mathbf{d}(\omega)$	$(VN \times 1)$ vector of the complex driving functions for all sources i per angular frequency ω
$D_{\text{in}}(i, \omega)$	(complex) signal input of the i-th source at the angular frequency ω
$D_{\text{opt}}(i, \omega)$	complex optimized filter of the i-th source at the angular frequency ω
$D_{\text{xo}}(\omega)$	complex frequency band crossover at the angular frequency ω
$E(\omega)$	frequency dependent absolute error between the obtained and the desired sound field in the audience zone
f	frequency
$f_{\text{LF, MF}}$	low/mid crossover frequency
$f_{\text{MF, HF}}$	mid/high crossover frequency
f_{start}	start frequency for the calculations
f_{stop}	stop frequency for the calculations
$G(m, i, \omega)$	scaled ATF from the i-th source to the m-th receiver position at the angular frequency ω
$\mathbf{G}(\omega)$	$(M \times VN)$ scaled ATF matrix for all sources i and for all receiver positions m at the angular frequency ω
$H1(\omega)$	frequency dependent standard deviation of the distance compensated SPLs of all audience positions
j	imaginary unit, $\text{j}^2 = -1$
$L_p(\omega, m)$	frequency and position index dependent SPL
$L_{p,\text{a,na}}(\omega)$	frequency dependent relation of the obtained average SPLs of the audience and the non-audience zone
$P(m, \omega)$	sound pressure at the m-th receiver position at the angular frequency ω
$P_{\text{des}}(m, \omega)$	desired sound pressure at the m-th receiver position at the angular frequency ω
$\mathbf{p}(\omega)$	$(M \times 1)$ vector of sound pressures at all receiver positions m at the angular frequency ω
$\mathbf{p}_{\text{des}}(\omega)$	$(M \times 1)$ vector of desired sound pressures at all receiver positions m at the angular frequency ω
p_0	reference sound pressure, $p_0 = 2 \cdot 10^{-5}$ Pa
$R(\beta, \omega)$	specific far-field radiation pattern for the radiation angle β at the angular frequency ω
$S(i, \omega)$	i-th loudspeaker sensitivity specifying the SPL in 1 m distance for 1 W electrical input power at the angular frequency ω
σ	standard deviation
ω	angular frequency

Table 3. List of variables—LSA setup and venue characteristics

i	index of the LSA loudspeakers, with $i = 1, 2, ..., VN$
K	number of sections of the PAL
k	index of the PAL section, with $k = 0, 1, 2, ..., K$
M	number of receiver positions in the vertical radiation plane, with $M = M_{\text{a}} + M_{\text{na}}$
M_{a}	number of audience positions in the vertical radiation plane
$\mathcal{M}_{\text{a}}$	set of audience positions in the vertical radiation plane
M_{na}	number of non-audience positions in the vertical radiation plane
$\mathcal{M}_{\text{na}}$	set of non-audience positions in the vertical radiation plane
M_{v1}	number of receiver positions in the vertical radiation plane of venue 1
M_{v2}	number of receiver positions in the vertical radiation plane of venue 2
m	index of the receiver positions, with $m = 1, 2, ..., M$
N	number of individual LSA cabinets and therefore also number of PAL segments
n	index of the LSA cabinet, with $n = 1, 2, ..., N$
V	number of vertically stacked loudspeakers per LSA cabinet (different for each frequency band)

Table 4. List of variables—lengths

Γ	total length of the covered PAL sections
Γ_0	total length of the PAL
Γ_e	tolerated difference of the total PAL length and the total length of the covered PAL sections
Γ_n	length of the n-th PAL segment, with $\Gamma_n = \Gamma_{n,1} + \Gamma_{n,2}$
$\Gamma_{n,1}$	distance from the top to the center position of the n-th PAL segment, i.e., the segment's upper partial length
$\Gamma_{n,2}$	distance from the center to the bottom position of the n-th PAL segment, i.e., the segment's lower partial length
Δ_n	distance from the center of the $(n + 1)$-th and the n-th LSA cabinet to the receiver positions (for WST)
Θ	radius of a baffled circular piston
Λ_y	height of a line piston
$\Lambda_{y,\mathrm{LSA}}$	front grille's height of a single LSA cabinet
$\Xi_{n,1}$	required distance from the top to the center position of the n-th PAL segment
$\Xi_{n,2}$	required distance from the center to the bottom position of the n-th PAL segment
$\tilde{\Xi}_{n,1}$	partial distance from the top to the center position of the n-th PAL segment
$\tilde{\Xi}_{n,2}$	partial distance from the center to the bottom position of the n-th PAL segment

Table 5. List of variables—vectors and room coordinates

x	room coordinate
$\mathbf{x}$	two-dimensional vector with $\mathbf{x} = (x, y)^{\mathrm{T}}$
$\mathbf{x_{0,i}}$	vector of the i-th LSA source's front grille center position
$\mathbf{x_{a,b,n}}$	vector of the bottom position of the n-th PAL segment
$\mathbf{x_{a,c,n}}$	vector of the center position of the n-th PAL segment
$\mathbf{x_{a,t,n}}$	vector of the top position of the n-th PAL segment
$\mathbf{x_{b,n}}$	vector of the bottom position of the n-th LSA cabinet
$\mathbf{x_{c,n}}$	vector of the (front grille) center position of the n-th LSA cabinet
x_{H}	x-coordinate of the top position of the uppermost LSA cabinet
$\mathbf{x_m}$	vector of the m-th receiver position
$\mathbf{x_{PAL,k}}$	vector of the stop position of the k-th PAL section
$\mathbf{x_{PAL,k-1}}$	vector of the start position of the k-th PAL section
$\mathbf{x_S}$	vector of the source position of the virtual line source
$\mathbf{x_{t,n}}$	vector of the top position of the n-th LSA cabinet
y	room coordinate
y_{H}	y-coordinate of the top position of the uppermost LSA cabinet
z	room coordinate

Table 6. List of variables—angles

α_n	splay angle between the $(n + 1)$-th and the n-th LSA cabinet
$\beta(m, i)$	radiation angle for the m-th receiver position from the i-th source
γ_n	tilt angle of the n-th LSA cabinet
ε_k	tilt angle of the k-th PAL section
ψ_n	coverage angle of the n-th LSA cabinet (for PALC)
$\tilde{\psi}_n$	n-th partial coverage segment angle of the PAL
ψ_{init}	initial coverage angle of the LSA cabinets

Table 7. Selected venue slice coordinates according to venue 1 from Fig. 2a.

m	x_m / m	y_m / m
1	0	−11
15	7	−11
101	50	−11
122	58.1492	−4.3788
131	58.1492	0.1212
152	66.2984	6.7424
165	66.2984	13.2424
297	0.2984	13.2424

Table 8 Selected venue slice coordinates according to venue 2 from Fig. 2b.

m	x_m / m	y_m / m
1	0	−10
21	10	−10
62	30.4426	−8.4668
231	110.0423	19.8906
246	110.0423	27.3906
466	0.0423	27.3906

Table 9 Splay angles α_n, source-to-receiver distances Δ_n and their product following WST criterion number four for venue 1 using the PALC2 tilt angles.

LSA cabinets	α_n / deg	Δ_n / m	$\alpha_n \cdot \Delta_n$ / (rad · m)
1...2	1.6	62.12	1.73
2...3	1.67	59.48	1.73
3...4	1.72	58.2	1.75
4...5	1.74	58.33	1.77
5...6	1.75	57.62	1.76
6...7	1.79	55.55	1.74
7...8	1.86	53.61	1.74
8...9	1.93	51.8	1.74
9...10	2.13	44.13	1.64
10...11	2.55	36.1	1.61
11...12	3.13	29.4	1.61
12...13	3.84	23.87	1.6
13...14	4.73	19.37	1.6
14...15	5.82	15.77	1.6
15...16	7.12	12.94	1.61

Table 10 Splay angles α_n, source-to-receiver distances Δ_n and their product following WST criterion number four for venue 2 using the PALC2 tilt angles.

LSA cabinets	α_n / deg	Δ_n / m	$\alpha_n \cdot \Delta_n$ / (rad · m)
1...2	1	95.55	1.67
2...3	1.11	86.23	1.67
3...4	1.24	77.71	1.68
4...5	1.37	69.95	1.67
5...6	1.53	62.88	1.68
6...7	1.7	56.47	1.68
7...8	1.89	50.68	1.67
8...9	2.11	45.45	1.67
9...10	2.35	40.75	1.67
10...11	2.62	36.55	1.67
11...12	2.92	32.8	1.67
12...13	3.39	27.6	1.63
13...14	4.12	22.07	1.59
14...15	5.15	17.64	1.59
15...16	6.43	14.16	1.59

Table 11 Tilt angles of the LSA cabinets for the geometry used in Fig. 1 and for venue 1 from Fig. 2a for the different curvings (arc, J, progressive, PALC1, PALC2, MA1, and MA2). Every cabinet of the straight array is tilted by 7 deg.

LSA	γ_n / deg	γ_n / deg	γ_n / deg	γ_n / deg	γ_n / deg	γ_n / deg	γ_n / deg
cabinet	arc	J	prog	PALC1	PALC2	MA1	MA2
1	−2	−1	−2	−1.53	−2.45	−3	−3
2	1	−1	−1.62	1.84	−0.85	−2.5	−2.5
3	4	−1	−0.85	5.2	0.82	−2	−0.5
4	7	−1	0.3	8.55	2.54	−1	0
5	10	−1	1.83	11.88	4.29	0	4
6	13	−1	3.75	15.19	6.04	1	6
7	16	−1	6.05	18.39	7.83	2	10
8	19	4	8.73	21.48	9.69	3	10.5
9	22	9	11.8	24.45	11.62	4	14.5
10	25	14	15.25	27.31	13.75	5	16.5
11	28	19	19.1	30.05	16.3	7	18.5
12	31	24	23.32	32.67	19.43	9	22.5
13	34	29	27.92	35.18	23.27	11	26.5
14	37	34	32.9	37.57	28.01	12	30.5
15	40	39	38.27	39.84	33.83	18	38
16	43	44	44	42	40.95	25.5	45.5

Table 12 Tilt angles of the LSA cabinets for the geometry used in Fig. 1 and for venue 2 from Fig. 2a for the different curvings (arc, J, progressive, PALC1, PALC2, MA1, and MA2). Every cabinet of the straight array is tilted by –4 deg.

LSA	γ_n / deg	γ_n / deg	γ_n / deg	γ_n / deg	γ_n / deg	γ_n / deg	γ_n / deg
cabinet	arc	J	prog	PALC1	PALC2	MA1	MA2
1	−7.14	−7	−7.1	–7.14	−8.24	−9.3	−8.8
2	−4.54	−7	−6.78	−4.03	−7.24	−8.8	−8.3
3	−1.94	−7	−6.13	−0.98	−6.12	−8.3	−7.8
4	0.66	−7	−5.15	2.01	−4.89	−7.8	−7.3
5	3.26	−7	−3.85	4.94	−3.51	−7.3	−5.3
6	5.86	−7	−2.23	7.81	−1.99	−6.8	−4.8
7	8.46	−7	−0.28	10.63	−0.29	−6.3	0.2
8	11.06	−7	2	13.39	1.6	−5.8	3.2
9	13.66	−2.13	4.6	16.09	3.71	−5.3	6.2
10	16.26	2.75	7.53	18.69	6.06	−3.3	9.2
11	18.86	7.63	10.78	21.18	8.68	−1.3	12.2
12	21.46	12.5	14.35	23.56	11.6	0.7	15.2
13	24.06	17.38	18.25	25.83	14.98	2.7	20.2
14	26.66	22.25	22.48	27.97	19.1	4.7	23.2
15	29.26	27.13	27.03	30	24.25	6.7	27.2
16	31.86	32	31.9	31.91	30.68	14.2	30.2

THE AUTHORS

Florian Straube

Frank Schultz

David Albanés Bonillo

Stefan Weinzierl

Florian Straube received the Dipl.-Ing. degree in electrical engineering/communications and information technology from Technische Universität Dresden in cooperation with Klippel GmbH in 2013. Since 2014 he has been working as a research associate at Audio Communication Group at TU Berlin focusing on sound field synthesis and line source array applications for sound reinforcement.

•

Frank Schultz received the M.Sc. in audio communication and technology from Technische Universität Berlin and the Dr.-Ing. degree with distinction from Universität Rostock, in 2011 and 2016, respectively. From 2003–2007 he worked at EVI Audio GmbH/Bosch Communications Systems, Straubing, as an audio DSP engineer. Since 2016 he has been working at sonible GmbH, Graz, as senior R&D engineer for 3D audio. Recent research interests are sound field synthesis applications and acoustic signal processing for loudspeaker arrays. He is currently a visiting postdoc at the Audio Communication Group at Technische Universität Berlin. He is a member of the AES and reviews for the AES and the IEEE.

•

David Albanés Bonillo received the M.Sc. degree in telecommunications engineering with a focus on digital signal processing from the Universidad Europea de Madrid in 2011. Since 2013 he has been working towards the M.Sc. in audio communication and technology from Technische Universität Berlin and is a research assistant at the TU Berlin. His fields of interest are electroacoustics, loudspeaker development, and digital signal processing.

•

Stefan Weinzierl is head of the Audio Communication Group at the Technische Universität Berlin. His activities in research are focused on audio technology, virtual acoustics, room acoustics, and musical acoustics. He is coordinating a master program in Audio Communication and Technology at TU Berlin and teaching Tonmeister students at the University of the Arts (UdK). With a diploma in physics and sound engineering and a two-year study in musicology at UC Berkeley, he received his Ph.D. from TU Berlin. He is coordinating research consortia in the field of virtual acoustics (SEACEN) and music information retrieval (ABC_DJ).